Angular magnetoresistance in the $(DMET\text{-}TSeF)_2X$ family: $(X=AuCl_2, AuI_2)$: Field-induced spin-density waves and commensurability effects

N. Biškup and J. S. Brooks
NHMFL, FSU, 1800 East Paul Dirac Drive, Tallahassee, Florida 32310

R. Kato
RIKEN, The Institute of Physical and Chemical Research, 2-1, Hirosawa, Wako-shi, Saitama 351-0198, Japan

K. Oshima
Department of Physics, Faculty of Science, Okayama University, Tsushima-naka, Okayama 700, Japan
(Received 19 January 2000)

We present a detailed study of angular-dependent magnetoresistance (AMR) in a class of low-dimensional organic conductor $(DMET\text{-}TSeF)_2X$, where X stands for $X=AuCl_2$ and AuI_2. The angular-dependent background magnetoresistance for both compounds reveals a local minimum at the angle where the field-induced spin-density wave (FISDW) at lowest field is observed, contrary to the standard quasi-one-dimensional systems like the Bechgaard salts. Both systems show commensurability effects of electron motion, reflected as a series of magnetoresistance dips in tilted magnetic field at Lebed magic angles. While commensurability effects in $AuCl_2$ dominate the FISDW, AuI_2 shows complicated AMR structure dominated by FISDW. These data indicate continuous sliding of the FISDW nesting vector in the *b-c* plane.

Quasi-one-dimensional (Q1D) organic conductors play an important role in the research of electronic interactions in solid state physics. The family of Bechgaard salts has been traditionally used to investigate magnetic Q1D instabilities, which result in spin density wave (SDW), and (magnetic) field induced spin density wave (FISDW) states. Quasi-one-dimensionality arises from the high anisotropy: tight binding calculations give transfer integral ratio of $t_a:t_b:t_c = 1:0.1:0.003$, giving a Fermi surface (FS) consisting of a pair of open, slightly warped sheets. Despite extensive studies in this family, many challenging questions remain open. This includes the complete understanding of quantum phenomena [FISDW states and rapid oscillations (RO)], commensurability effects (including Lebed angles), and even basic concepts of electronic structure (Fermi or Luttinger liquid).

The high anisotropy leads to the instabilities which yield either SDW or FISDW states.[1] In both cases one Q1D Fermi sheet is nested to its counterpart by a nesting vector $Q(Q_a,Q_b,Q_c)$. The strict 2D theoretical model predicts the best SDW nesting vector $Q=(2k_F,\pi/b)$, k_F being Fermi wave vector and a,b,c crystal axes. However, experimental data reveal that the nesting is three dimensional, that is, $Q=(2k_F,\pi/2b,\pi/8c)$ where Q_b is reduced and Q_c is not zero.[2] We will show that a finite Q_c can introduce additional, effects beyond the 2D approximation. The previous reports of unusual angular behavior of FISDW and RO amplitude,[3,4] also indicate that third direction plays a more significant role than predicted by the simple 2D model. In systems with more pronounced FS warping, when the intrinsic 1D SDW instability is suppressed, FISDW states are obtained. In 1984 Gor'kov and Lebed'[5] showed that in such systems magnetic field (B) can restore the SDW which leads to series of quantized magnetic field induced SDW (FISDW) phase transitions. Montambaux's finite-temperature calculations[6] gave logarithmic divergence of magnetic susceptibility χ(B) periodic in 1/B. Calculations are made for a 2D electron gas with quantized FISDW nesting vector Q given by $Q=(2k_F+ebBn,\pi/b)$ with third direction omitted. However, even in this strictly 2D model, $\chi(B)$ is quantized only in the a-direction (best conducting axis), showing that the divergence peak continuously develops in the perpendicular direction inside a single quantum state n (see Fig. 3 in Ref. 6).

Angular magnetoresistance (AMR) measurements appear to be one of the very useful methods to study organic Q1D systems since AMR is affected by both FISDW and commensurability effects. The latter are shown to arise at certain angles of incident magnetic field in respect to the crystal axis. The first theoretical predictions in 1989 by Lebed and Bak[7] were soon followed by experimental reports of commensurability effects in Bechgaard salts.[8,9] Several different theoretical interpretations in following years succeeded to explain the appearance of dips (instead of peaks as originally proposed in Ref. 7) in the framework of Fermi liquid theory. Osada *et al.*[10] showed that the semiclassical Boltzmann equation in highly anisotropic systems gives dips in the resistivity in all three crystal axis directions as observed experimentally.[11,10] On the other hand, the AMR data in Ref 9 were interpreted as a consequence of the non-Fermi liquid.[12]

To gain new insight in this problem beyond the highly studied Bechgaard salts, we have examined a class of organic materials, the $(DMET\text{-}TSeF)_2X$ family (where X stands for $AuCl_2$, AuI_2, $AuBr_2$, I_3). These materials are organic charge transfer salts with a hybrid donor molecule (DMET-TSeF).[13] The anions are linear and therefore do not induce anion ordering which can screen or influence the low-temperature properties. Tight binding calculations at room temperature give a Q1D Fermi surface consisting of a pair of

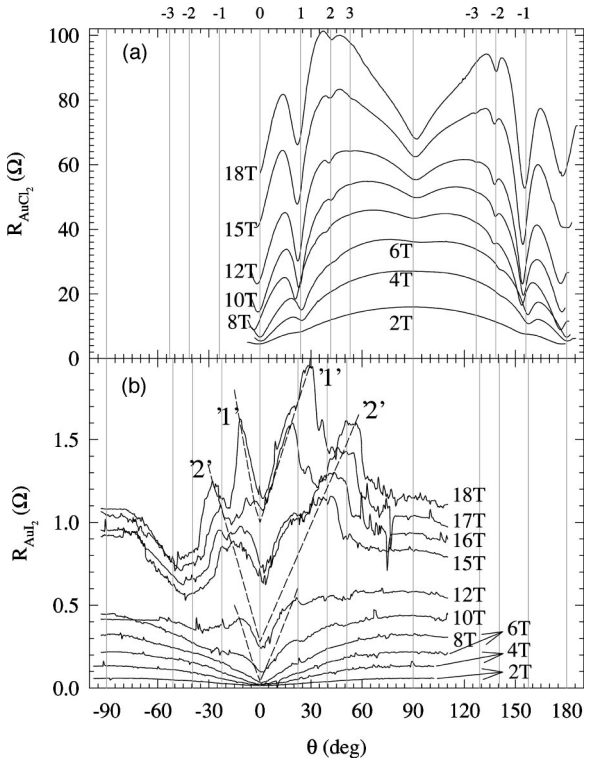

FIG. 1. Angular dependence of magnetoresistance for different magnetic fields. θ is the angle of the magnetic field from the b axis. Vertical lines represent the Lebed angles calculated from the lattice parameters and labeled as p/q according to Eqs. (2). (a) $(DMET\text{-}TSeF)_2AuCl_2$. (b) $(DMET\text{-}TSeF)_2AuI_2$. Numbers in quotes indicate the FISDW index corresponding to each maxima. Broken lines are guides for the eye for the shift of these maxima.

open, slightly warped sheets very similar to the Bechgaard salts.[13] Here we present and compare AMR data of two members of this new family: $(DMET\text{-}TSeF)_2AuCl_2$ and $(DMET\text{-}TSeF)_2AuI_2$ (hereafter referred to as $AuCl_2$ and AuI_2). Both are metallic, but only AuI_2 becomes superconducting at $T=0.58$ K. Despite the lack of superconductivity in $AuCl_2$ (at least above 25 mK), the Q1D instability appears in both cases at *ambient pressure*: at moderate magnetic field (B), FISDW transitions are reported.[14,3]. Rapid oscillations (RO) ($F_{SDW}\cong 300$ T) are also detected in both systems.[3,15] In this paper, we report a significant difference in AMR data in these two related compounds.

The procedure of synthesis is described in Ref. 13. Single crystals of approximately $1\times0.1\times.01$ mm^3 for the $AuCl_2$ and $0.5\times0.05\times0.01$ mm^3 for the AuI_2 compound are mounted on a sample rotator and contacted with 12.5 μm golden leads. The ac current is applied along the a axis, while magnetic field rotated in the b-c plane. Here we note that b and c axis are switched compared to Bechgaard salt: the longest unit cell direction is the b axis. For $B\|b$, the FISDW occurs at the lowest threshold field. The data are taken in both dilution refrigerator for temperatures up to 600 mK and in a regular helium cryostat for higher temperatures. Three different AuI_2 samples, and five different $AuCl_2$ samples were investigated.

Figures 1(a) and 1(b) show the resistance $R_a(B)$ versus angle θ for $(DMET\text{-}TSeF)_2AuCl_2$ and $(DMET\text{-}TSeF)_2AuI_2$ samples, respectively, at $T=25$ mK. θ is the angle in the b-c plane measured between the b axis and the magnetic field. In order to avoid nonlinear effects in the FISDW states, low ac currents of 10 and 5 μA for $AuCl_2$ and AuI_2 sample, respectively, is applied. In both cases, FISDW transitions are detected for $B\|b$, i.e., at $\theta=0°$ and 180° where an absolute minimum appears at all fields. No FISDW is obtained for $B\|c$. The vertical lines indicate Lebed's magic angles with indices given in the figure. For the triclinic symmetry in the present case, the simple condition $\tan(\theta)=(p/q)(c/b)$ is modified to

$$\tan(\theta)=\frac{p}{q}\frac{c}{b}\frac{\sin\beta}{\sin\gamma\sin\alpha}-\cot\alpha \tag{1}$$

which gives

$$\tan_{AuCl_2}\theta=0.442\frac{p}{q}\ \text{ and }\ \tan_{AuI_2}\theta=0.412\frac{p}{q}, \tag{2}$$

taking lattice parameters from Ref. 13, and neglecting the $\cot\alpha$ term. In the $AuCl_2$ sample, the $p/q=1$ dip is extremely pronounced and observable down to the lowest fields. Dips are observed for all values of magnetic field in both normal and FISDW phases without visible difference. The wide dip around $B\|c$ is a consequence of the FISDW: at angles far from the $B\|b$ direction, the FISDW is suppressed due to usual $(1/\cos\theta)$ 2D orbital dependence[3] and the resistance decreases.

In the case of the AuI_2 sample, the situation is more complicated. Figure 1(b) shows one of the samples with the lowest resistance which can account for the considerable noise. In addition to the pronounced $p/q=0$ dip, AuI_2 shows only a slight trace of the $p/q=\pm1$ dip (compared with much larger effects in $AuCl_2$). Furthermore, additional peak structure appears at angles between 0° and 90°, and resembles data in $(TMTSF)_2ClO_4$.[16] These peaks start to appear at fields higher than 8 T, and shift with increasing B. (The angular asymmetry of these peaks is observed in certain extent also in other samples measured and can be understood as a consequence of small misalignment of crystal axis in a magnetic field.) However, in all cases the angular position of peaks shows a linear dependence with magnetic field above the 8 T threshold field. This coincides with the appearance of FISDW, which is the origin of these anomalies. We note that this complicated AMR structure does not scale with $B\cos\theta$, and therefore cannot be explained as the effective transverse magnetic field perpendicular to the a-c plane. This is reflected in a significant difference between sweeps of resistance vs magnetic field at $\theta=0°$ and resistance vs angular dependence at constant B. This AMR picture is found in all three measured AuI_2 samples. We will return to this problem in the final discussion.

In Fig. 2 we replot the $B=2$ T curves from Fig. 1 for both materials. At this small field no FISDW is present. In the case of $AuCl_2$ sample, the signature of the $p/q=\pm1$ is observable, showing that commensurability structure in this material is independent of the FISDW formation. In both cases, data are well fitted to a $\sin^{1/2}\theta$ behavior in the region around 90° ($B\|c$). AuI_2 at higher fields (4 to 8 T) indicates change to pure sinusoidal dependence, while in $AuCl_2$ the Lebed dips distort the background AMR curve already at $B=4$ T. This resembles the behavior observed in

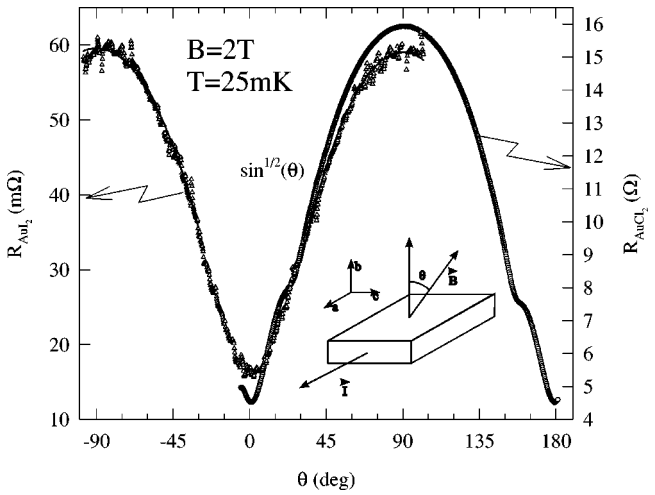

FIG. 2. Low field ($B=2$ T) AMR for AuI_2 (triangles, left) and $AuCl_2$ (circles, right). Fits in the region around $\theta=90°$ have a $\sin^{1/2}\theta$ dependence. Inset shows the geometrical arrangement of the experiment.

$(TMTSF)_2ClO_4$ and $(TMTSF)_2PF_6$,[16,9] but shifted by 90°: in Ref. 9 the background was approximated by $\cos\theta$ behavior with indications of $\cos^{1/2}\theta$ at low fields. The sinusoidal AMR dependence in (DMET-TSeF) family is different from the behavior in the Bechgaard salts: in the latter only the component of B along the least conducting axis is important. This is attributed to (in)coherent hoping between conducting chains. In our case, the least conducting direction does not match with the direction in which FISDW is observed, which implies the necessity to reconsider the current understanding of AMR in organic conductors.

Figure 3 shows the position of successive FISDW transitions found in AuI_2 at 25 mK. The data are extracted from the change of MR slope. At 8 T the first detectable change occurs, which we estimate as the FISDW threshold field. These transitions are not strictly periodic in $1/B$, which is also the case for some of the Bechgaard salts.[1] We have labeled successive phases by integer numbers in spite of their irregularity, assuming some similarity with $AuCl_2$ sample.[3] It seems that this irregularity is connected with the unusual AMR picture [Fig. 1(b)]. In contrast, for $AuCl_2$, the FISDW are periodic in $1/B$ and the AMR are dominated by the Lebed

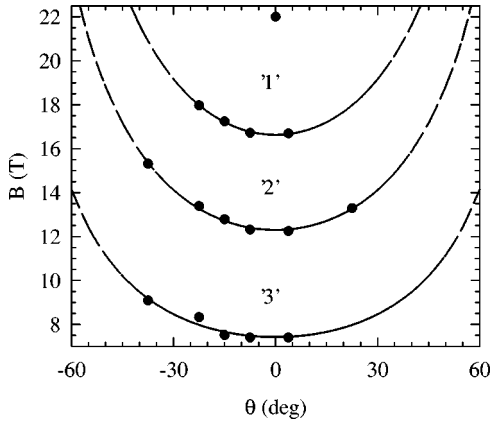

FIG. 3. Angular dependence of FISDW transitions in $(DMET\text{-}TSeF)_2AuI_2$. Lines are fits to $1/\cos\theta$ dependence.

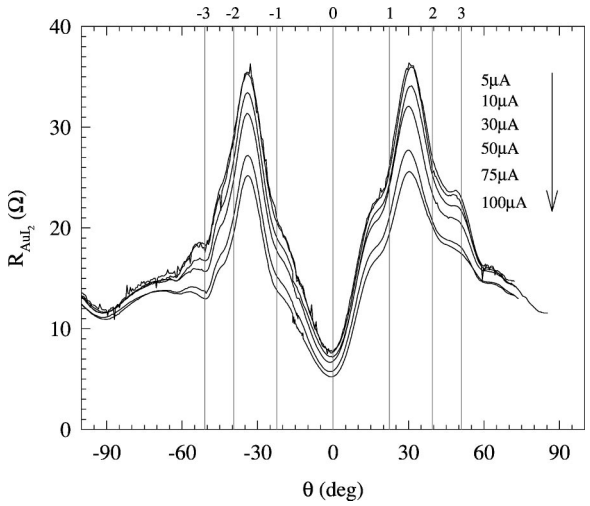

FIG. 4. AMR of $(DMET\text{-}TSeF)_2AuI_2$ sample for different currents. Vertical lines indicate Lebed angles, labeled p/q according to Eq. (2).

oscillations. On the other hand, FISDW steps in Fig. 3 follow the usual 2D orbital dependence. Lines are fits to $1/\cos\theta$ dependence similar to observed in $AuCl_2$.[3] The consequences of these transitions are discussed below.

Figure 4 shows the AMR data in AuI_2 for different currents. This is a different sample studied at $T=40$ mK and $B=17.8$ T. One can again observe a local MR maximum at certain angle in the b-c plane and also Lebed resonances with indexes $p/q=\pm1,2,3$. The higher the current, the more pronounced the Lebed dips become. The main point in this figure is the angular distribution of the nonlinear effects in this material. Nonlinear resistance arises due to sliding of the FISDW condensate. At zero electric field the condensate is pinned by impurities but after a finite electric threshold field E_T is applied, it is depinned and contributes to the electrical conductivity.[17] E_T in our systems is found to be few mV/cm, comparable to E_T's in Bechgaard salts. One can observe that there is no non-linearity (within experimental error) for $\theta=\pm90°$, i.e., at $B\|c$ (note: this is an angle where no FISDW is detected). The nonlinearity appears at angles close to 0° and reaches its absolute maximum at the local MR maximum. This suggests that these MR maxima are a consequence of the FISDW. If one recalls that the increase of resistance is an indication of FS nesting, one can conclude that the best FS nesting occurs at a finite angle in the b-c plane.

If we look again to the shift of these local maxima in Fig. 1(b), we can conclude that the FISDW nesting vector shifts with increasing magnetic field. Broken lines in Fig. 1(b) are guides to the eye of the shift of these maxima with field: starting points ($\theta=0$) correspond to $B=8$, 12.3, and 16.6 T FISDW transitions, as deduced from Fig. 3. This shift appears to be continuous. To our knowledge this is the first observation of a continuous shift of nesting vector in the perpendicular (b-c) plane. One can assign two low-angle peaks at 17 and 18 T in Fig. 1(b) as a FISDW vector shift in the $n=1$ state. With increasing angle, the system drops back to the $n=2$ state leading to a reappearance of the previous peaks. This implies that Q vector shifts in the b-c plane following the best nesting condition inside the quantized FISDW state. Once the field reaches a critical value, a quan-

tized step of Q_a occurs and sliding in the b-c plane recovers again. This reveals the importance of the third axis in these systems, previously treated as purely 2D. However, we note that even in the 2D model,[6] the FISDW nesting vector is quantized only in the longitudinal direction and has broad continuous maxima in the perpendicular direction. Further, it is intriguing to consider the difference between $AuCl_2$ and AuI_2. In the former, FISDW transitions are regular and no irregularity in AMR is observed. In the latter FISDW transitions are not uniform in $1/B$ and continuous shift of the FISDW nesting vector in the b-c plane is observed. This reveals that the deviation from the standard 2D description is influenced by the third axis effect. We emphasize the similarity between AuI_2 and $(TMTSF)_2ClO_4$,[16] which is another system with irregular FISDW transitions.

In summary we report AMR effects in a class of Q1D organic materials $(DMET\text{-}TSeF)_2AuCl_2$ and $(DMET\text{-}TSeF)_2AuI_2$. Contrary to the case of $(TMTSF)_2PF_6$, the $\theta=0°$ orientation (along the b axis where FISDW is observed) is not the least conducting direction in finite magnetic field. This shifts the low-field MR dependence to a $\sin\theta$ behavior. Nonlinear conductance due to sliding of FISDW condensate above a small E_T is observed in both compounds. AMR in $(DMET\text{-}TSeF)_2AuI_2$ closely resembles the case of $(TMTSF)_2ClO_4$, with the appearance of local MR maxima in a b-c plane. These maxima shift linearly in a magnetic field above the FISDW threshold field, implying a continuous shift of the FISDW nesting vector in the b-c plane.

This work was supported by Grant No. NSF-DMR-99-71474. The NHMFL is supported through a contractual agreement between the NSF through Grant No. NSF-DMR-95-27035 and the State of Florida.

[1] For an overview of low dimensional phenomena see T. Ishiguro, K. Yamaji and G. Saito, *Organic Superconductors*, 2nd ed. (Springer Verlag, Berlin, 1997).

[2] T. Takahashi, Y. Maniwa, H. Kawamura, and G. Saito, Physica B **143**, 417 (1986); J. M. Delrieu, M. Roger, Z. Toffano, E. Wope Mbougue, R. Saint James, and K. Bechgaard, *ibid.* **143**, 412 (1986).

[3] N. Biškup, J. S. Brooks, R. Kato, and K. Oshima, Phys. Rev. B **60**, 15 005 (1999).

[4] G. S. Boebinger, G. Montambaux, M. L. Kaplan, R. C. Haddon, S. V. Chichester, and L. Y. Chiang, Phys. Rev. Lett. **64**, 591 (1990).

[5] L. P. Gor'kov and A. G. Lebed', J. Phys. (France) Lett. **45**, 433 (1984).

[6] G. Montambaux, M. Héritier, and P. Lederer, Phys. Rev. Lett. **55**, 2078 (1985).

[7] A. G. Lebed and P. Bak, Phys. Rev. Lett. **63**, 1315 (1989).

[8] T. Osada, A. Kawasumi, A. Kagoshima, N. Miura, and G. Saito, Phys. Rev. Lett. **66**, 1525 (1991).

[9] W. Kang, S. T. Hannahs, and P. M. Chaikin, Phys. Rev. Lett. **69**, 2827 (1992).

[10] T. Osada, S. Kagoshima, and N. Miura, Phys. Rev. Lett. **77**, 5261 (1996).

[11] G. M. Danner, W. Kang, and P. M. Chaikin, Phys. Rev. Lett. **72**, 3714 (1994).

[12] S. P. Strong, D. G. Clarke, and P. W. Anderson, Phys. Rev. Lett. **73**, 1007 (1994).

[13] R. Kato, S. Aonuma, Y. Okano, H. Sawa, M. Tamura, M. Kinoshita, K. Oshima, A. Kobayashi, K. Bun, and H. Kobayashi, Synth. Met. **61**, 199 (1993).

[14] K. Oshima, H. Okuno, and R. Kato, Synth. Met. **70**, 861 (1995).

[15] N. Biškup (unpublished).

[16] M. J. Naughton, O. H. Chung, M. Chaparala, X. Bu, and P. Coppens, Phys. Rev. Lett. **67**, 3712 (1991).

[17] For an overview of nonlinear effects in Bechgaard salts see S. Tomić, J. R. Cooper, W. Kang, D. Jérome, and K. Maki, J. Phys. I **1**, 1603 (1991).